Picosecond discharges and stick–slip friction at a moving meniscus of mercury on glass

R. Budakian, K. Weninger, R. A. Hiller, S. J. Putterman

Physics Department, University of California, Los Angeles, California 90095, USA

At a meeting of the French Academy in 1700, Bernoulli demonstrated that swirling mercury in an evacuated flask generates light[1,2]. He emphasized that this 'barometer light' "has not been explained since its discovery about 30 years ago" by Picard[3]. Here we revisit this phenomenon and find that the repetitive emission of light from mercury moving over glass is accompanied by the collective picosecond transfer of large numbers of electrons. When brought into contact with mercury, the glass acquires a net charge. This charge separation provides a force which, in our experiment in a rotating flask, drags mercury against gravity in the direction of the motion of the glass. Eventually the edge of the mercury slips relative to the glass, accompanied by a picosecond electrical discharge and a flash of light. This repetitive build-up and discharge of static electricity thus gives rise to stick–slip motion. The statistics of the intervals between events and their respective magnitudes are history-dependent and are not yet understood.

Figure 1 shows a photograph of the apparatus used for these measurements. A cylindrical glass cell is sealed and mounted so that its axis lies in the horizontal plane perpendicular to the direction of gravity. It is filled to ~10% of its volume with mercury and in this case sealed in a neon gas atmosphere at a pressure of 340 torr. In our experiments this cell is rotated about its axis at a constant speed. As seen in the photograph light is emitted all along the line of contact of the mercury and the glass on the side where the glass leaves the mercury. Rough estimates indicate a power of 20 nW per centimetre of meniscus at a speed of rotation of 1 cm s^{-1} at the wall. This emission is easily seen with the unaided eye.

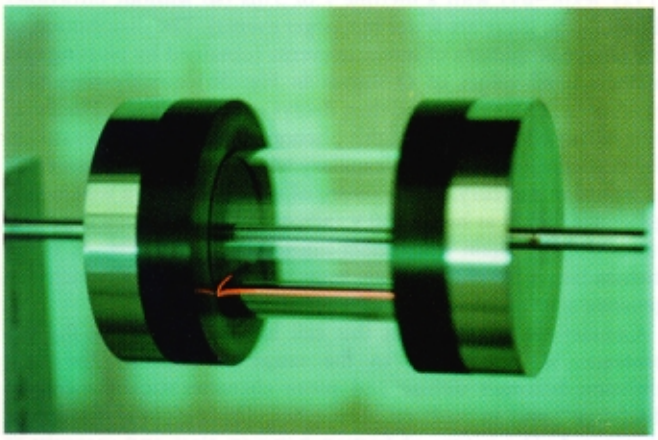

Figure 1 Photograph of the "barometer light", which is the orange line of light generated at the intersection of the mercury meniscus and the wall of the rotating glass cylinder. The rotation speed is 30° s^{-1}; the cylinder is made from Supracil with a wall thickness of 1 mm, a length of 5 cm, and an outer diameter of 2 cm. The cell is filled with 15 ml of mercury and above the mercury is neon gas at 340 torr. The light is emitted on the side where the wall leaves the mercury. With dimmed ambient lighting this effect is easily seen with the unaided eye, provided that the mercury is properly cleaned. Each black Delrin endcap is joined to the glass with an O-ring seal. We note that the Delrin–mercury interface also emits light.

Measurements were carried out using (1) a photomultiplier tube to resolve the temporal properties of the light, (2) a video camera to follow the line of contact between the mercury and glass, and (3) a capacitor (consisting of the 1-mm-diameter central conductor of an RG58 coaxial cable, with the shield cut parallel to the tip, pointing at the meniscus from the outside of the cell) to measure the charge transfer. The data shown in Fig. 2 were obtained using a nitrogen atmosphere (110 torr) above the mercury. In Fig. 2a, circles show the time dependence of the height of a 3-mm segment of the line of contact of the mercury and the glass; the electrical signals recorded by the capacitor are shown by vertical lines in this figure. Our key finding is that between electrical discharge events the mercury is moving in the direction of the glass (Fig. 2a) with a constant vertical velocity and that every discharge event, (which can have

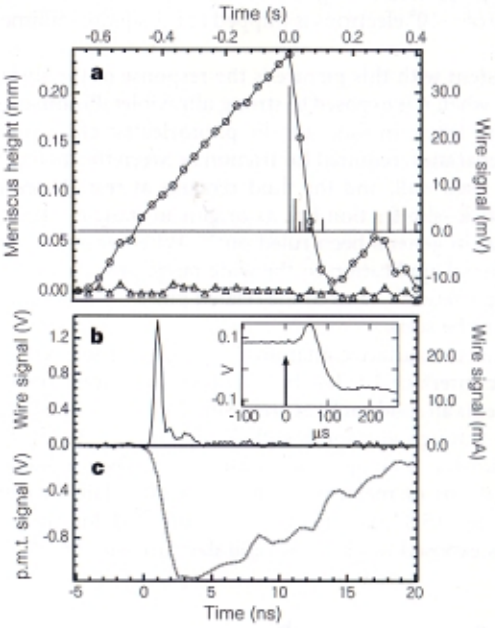

Figure 2 Correlation between stick–slip friction and picosecond electrical discharges at a glass–mercury interface. The Supracil cell is sealed with nitrogen at 110 torr and is rotated at 3° s^{-1} by a stepper motor acting through a 10 : 1 gear reduction. The meniscus motion in a 3 mm × 3 mm region is magnified ×20 and imaged by a Cohu CCD camera. In **a**, circles indicate the meniscus height as a function of time as read off the digitized frames which are acquired at the rate of 30 per s. Also shown in **a**, keyed to the right-hand vertical axis, are the electrical discharges recorded by the capacitor probe placed near the region of the cell being imaged. The discharge from the wire is here broadened in time using a 100 KΩ terminating resistor, and digitized to memory at 4 kHz. The key conclusion to be drawn from the data in this figure is that macroscopic stick–slip events are always accompanied by collective electrical discharges and, as shown in **b**, the timescale for the electrical events is measured in picoseconds. To obtain the picosecond resolution displayed **b** the instantaneous voltage was acquired with a Tektronix 684B digital oscilloscope working at 5×10^9 samples per second with a 50 Ω termination. The lower trace in **a** indicated by the triangles displays the surface motion when a deuterium lamp illuminates the entire surface with broadband ultraviolet light. In this case both electrical discharges and the stick–slip motion are suppressed. The inset in **b** shows a qualitative measure of the ~100 μs hydrodynamic timescale for meniscus motion to be completed after the discharge event (indicated by the arrow). A position-sensitive photodector records laser light scattered off the meniscus (for this data the rotation rate is 5° s^{-1}). The timescale for light emission by the nitrogen gas that has been excited by the electrical discharge is determined by a photomultiplier tube (p.m.t.) with a rise time of 650 ps as shown in **c**. Light is collected from the mercury–glass interface using a 800-μm silica fibre which then channels it to the photodetector which is sufficiently removed so as to minimize cross-talk between its anode and the electrical discharge.

an instrument-limited rise time of 375 ps; Fig. 2b) is followed by a sudden fall in the height of the mercury. The scattering of laser light directed at the curved meniscus indicates that the hydrodynamic response of the fluid surface to the discharge-triggered slip (indicated by the arrow in Fig. 2b inset) takes ~100 μs to be completed.

Our picture of the process is as follows: as portions of the glass come into contact with the mercury, electrons hop to sites on the glass where they remain as the glass separates from the mercury. This trapped static charge exerts a force on its image in the mercury which is strong enough to drag the fluid along until a sudden discharge releases this force, allowing the mercury to fall. Acquisition of the signal shown in Fig. 2b is made possible by the fact that the separated charge induces an image charge on the capacitor probe as well as in the mercury. When the discharge occurs, the capacitor discharges to ground through a 50 Ω resistor, producing the voltage plotted in Fig. 2b. According to this measurement, a charge Q of $\sim 10^6$ electrons is trapped in the square millimetre being probed.

Consistent with this picture is the response of the surface of the mercury when it is exposed to strong ultraviolet illumination from a deuterium lamp. In this case the photoelectric effect prevents the charge separation required for friction between the mercury and the rotating glass wall, and the fluid remains at rest. At least for this system stick–slip friction has its origins in static electricity, a view which has in general been ruled out[4,5]. Whether our results have a more general application to the wide range of systems that display stick–slip friction[6,7] (and to the related phenomenon of polishing[8]) remains to be seen.

The effect of surface contaminants on interactions at a mercury–dielectric interface[5,9–11] has been known for a long time[12]. In our experiments all solid surfaces are cleaned with acetone. Dripping the mercury through acetone is sufficient to render the light-emitting state attainable. To reprodicibly observe the effects reported here we allowed drops of mercury from a pipette to fall through a 25% solution of (15.8 M) nitric acid in water[13]. If the mercury–glass system is exposed to air for several days, the size of the individual discharge events increases at first. For still older mercury the "barometer light" disappears, an effect which delayed the acceptance of Bernoulli's demonstrations[14].

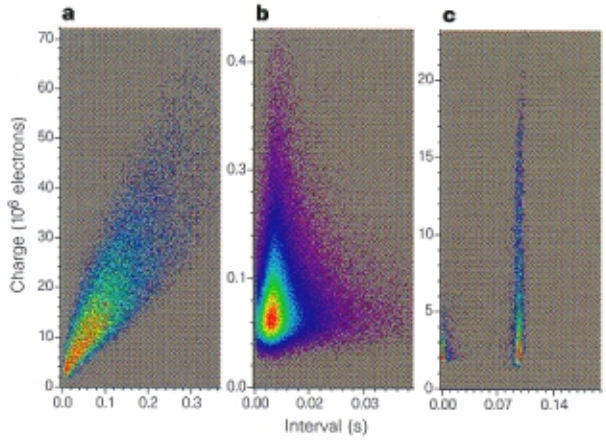

Figure 3 Plot of discharge events in terms of the time to the next event and its strength. The distribution of discharge events is obtained for: **a**, a Supracil quartz cell sealed with nitrogen at 110 torr rotating at 5° s^{-1}; and **b**, the same arrangement (rotating at 2° s^{-1}) but subjected to illumination with ultraviolet light. The intensity of illumination is substantially less than was used to suppress stick–slip friction in Fig. 2a. In **c** is displayed the distribution for events generated by a 1-cm-long glass capillary of 2-mm outer diameter fused over platinum wire which oscillates vertically at 10 Hz in a pool of mercury in a 200 torr neon atmosphere. In **a** and **b** the signal across 1 MΩ is amplified and low-pass-filtered before being digitized. The noise level after filtering the 60 Hz component is one-seventh of the trigger level. Data is acquired for ~1 h and the rate of (the smaller) events in **b** is over ten times greater than in **a**. In **c** is displayed the result of 7,200 events. In all panels, the density of points is highest for red and lowest for purple.

The barometer light can be compared to sonoluminescence[15–17] in that each involves the conversion of mechanical stress (rotation or sound) into light. The spectra, however, are different: the latter are broad band without lines, and the former are dominated by the emission lines of the surrounding gas[15–18]. The phenomena are similar in that both are triggered by a collective picosecond process.

Figure 3a shows the distribution of the size of events as a function of the time between them. These data indicate that a longer time between events implies a larger size for the next event, characteristic of earthquake statistics[19–21]. By summing all possible discharge sizes Q for a fixed time t between events, one finds that the probability per second of the next event has the form $(t/\tau^2)\exp(-t/\tau)$ where $\tau \approx 60$ ms. From the rotation rate (5° s^{-1}) and the cell diameter, this lifetime determines a characteristic length $\zeta \approx 50$ μm. Assuming that ζ determines the surface charge density ($\sigma \approx Q/\zeta^2$) makes the observed electrical discharge consistent with the well known equations of gas-discharge physics[18,22–24]. That is, the resulting electric field $E \approx \sigma/\epsilon_0$ where ϵ_0 is the electrical permittivity of vacuum, is sufficient to accelerate an electron to the ionization energy χ of a gas atom, typically 10 eV, in a mean free path l (that is, $eEl \approx \chi$, where e is the charge on an electron, $l \approx (p_0/p)$ μm, p_0 is 1 atm, and p is the gas pressure in the cell). The collisions between the accelerated electrons and the surrounding gas leave the atoms/molecules in excited states. Light-emitting transitions from these states have lifetimes ranging well into nanoseconds, as shown in Fig. 2c. Although the existence of the discharge is consistent with established theory we propose that the following processes remain unexplained: (1) the mechanism of charge transfer from mercury to the glass[25,26] (tunnelling has been suggested[27,28]); (2) the distribution of the excess charge on the glass (that is, the characteristic length ζ) which accounts for the 'static cling', discharge and slip events; and (3) the picosecond quenching of the charge separation.

In Fig. 3b we show the distribution of events for the case where the fluid is illuminated with ultraviolet light that is strong enough to affect the motion but is not as intense as was used to suppress friction as shown in Fig. 2a. In this case the illumination can be adjusted so that the events are markovian. The intrinsic process that controls the distribution gives in Fig. 3b has the form $(t^2/2\tau^3)\exp(-t/\tau)$ with a lifetime τ of 3 ms (so without ultraviolet illumination there are fewer but larger events). The distribution of the charge amplitude of intrinsic events (obtained by plotting as a histogram all values of Q shown in Fig. 3b) quickly rises to a maximum at $Q_0 \approx 10^5 e$ and then decays as $\exp(-2Q/Q_0)$. Finally, as part of our effort to control this phenomenon, we have vibrated in the vertical direction a glass capillary which has one end immersed in a pool of mercury. In the centre of the capillary is a wire which generates signals as high as 30 V (across 50 Ω) with picosecond rise times that are again instrument-limited. Shown in Fig. 3c is the distribution of events for this means of using triboelectricity to generate a string of picosecond electrical pulses.

Contact electrification in this cell is also affected by the gas pressure. When reduced to the range of 30 mtorr the light emission becomes diffuse and more characteristic of a corona discharge[29] and in such an atmosphere the stick–slip friction is eliminated. The nature of friction between glass and mercury at lower pressures (say 5 mtorr)—where well controlled experiments[28] have shown that large charge separations can build up as a result of the contact between surfaces—is beyond the capabilities of our current experiment.

Our measurements show that for mercury sliding on glass, stick–slip friction is due to the build-up of electric charge and its subsequent neutralization on a picosecond timescale. Small fluid velocities can generate a continuous stream of events (20 cyclings of charge per second at 2 minutes per revolution). This may be an ideal

system to study contact electrification and the formative time of sparks[22–24]. We propose that picosecond frictional-electricity may yield a useful characteristic of surfaces. One can wonder if liquid helium rubbing against caesium would display these effects. □

Received 25 March; accepted 7 October 1997.

1. Bernoulli, J. I. Sur le phosphore du baromètre. *Histoire Acad. Roy. Paris* 5–8 (1700); 1–8 (1701).
2. Harvey, E. N. *A History of Luminescence* (Am. Philosophical Soc., Philadelphia, 1957).
3. Picard, J. Sur la lumière du baromètre. *Mem. Acad. Roy. Sci.* **2**, 202–203 (1676).
4. Krim, J. Friction at the atomic scale. *Sci. Am.* **275**, 48–51, 54–56 (1996).
5. Harper, W. R. *Contact and Frictional Electrification* (Clarendon, Oxford, 1967).
6. Bowden, F. P. & Tabor, D. *The Friction and Lubrication of Solids* (Clarendon, Oxford, 1986).
7. Bhushan, B., Israelachvili, J. N. & Landman, U. Nanotribology: friction, wear and lubrication at the atomic scale. *Nature* **374**, 607–616 (1995).
8. Rabinowicz, E. *Friction and Wear of Materials* (Wiley, New York, 1965); Polishing. *Sci. Am.* **218**, 91–99 (1968).
9. Kemball, C. The adsorption of vapours on mercury. IV. Surface potentials and chemisorption. *Proc. R. Soc. Lond. A* **201**, 377–391 (1950).
10. Hays, D. A. in *Conference Series No. 48* 265–272 (Conf. Ser. No. 48, Inst. Phys., 1979).
11. Dybwad, G. L. & Mandeville, C. E. Generation of light by the relative motion of contiguous surfaces of mercury and glass. *Phys. Rev.* **161**, 527–532 (1967).
12. Rayleigh, Lord Experiments upon surface-films. *Phil. Mag.* **33**, 363–373 (1892).
13. *Handbook of Chemistry and Physics* 2989 (Chemical Rubber, Cleveland, 1954).
14. Bernoulli, J. I. Nouvelle maniere de rendre les baromètres lumineux. *Mem. Acad. Roy. Paris* 178–190 (1700).
15. Barber, B. P. & Putterman, S. J. Observation of synchronous picosecond sonoluminescence. *Nature* **352**, 318–320 (1991).
16. Hiller, R. A., Putterman, S. J. & Barber, B. P. Spectrum of synchronous picosecond sonoluminescence. *Phys. Rev. Lett.* **69**, 1182–1184 (1992).
17. Barber, B. P. *et al.* Defining the unknowns of sonoluminescence. *Phys. Rep.* **281**, 65–143 (1997).
18. Meek, J. M. & Craggs, J. D. (eds) *Electrical Breakdown of Gases* (Wiley, New York, 1978).
19. Carlson, J. M., Langer, J. S. & Shaw, B. E. Dynamics of earthquake faults. *Rev. Mod. Phys.* **66**, 657–670 (1994).
20. Demirel, A. L. & Granick, S. Friction fluctuations and friction memory in stick-slip motion. *Phys. Rev. Lett.* **77**, 4330–4333 (1996).
21. Burridge, R. & Knopoff, L. Model and theoretical seismicity. *Bull. Seismol. Soc. Am.* **57**, 341–371 (1967).
22. Rees, J. A. *Electrical Breakdown of Gases* (Macmillan, New York, 1973).
23. Penning, F. M. *Electrical Discharges in Gases* (Cleaver Hume, London, 1957).
24. Loeb, L. B. *Fundamental Processes of Electrical Breakdown in Gases* (Wiley, New York, 1939).
25. Moore, A. D. *Electrostatics* (Doubleday, New York, 1968).
26. Terris, B. D., Stern, J. E., Rugar, D. & Mamin, H. J. Contact electrification using force microscopy. *Phys. Rev. Lett.* **63**, 2669–2672 (1989).
27. Lowell, J. Tunnelling between metals and insulators and its role in contact electrification. *J. Phys. D* **12**, 1541–1554 (1979).
28. Kwetkus, B. A., Sattler, K. & Siegmann, H.-C. Gas breakdown in contact electrification. *J. Phys. D* **25**, 139–146 (1992).
29. Raizer, Y. P. *Gas Discharge Physics* (Springer, Berlin, 1991).

Acknowledgements. We thank L. Knopoff, T. Erber, J. Raffelski, G. Morales, S. Cowley, R. Löfstedt and P. H. Roberts for discussions, and E. Adams and C. Hiller for archival assistance. This work was supported by the US NSF and the US Department of Energy.

Correspondence should be addressed to S.J.P.